

RESEARCH ARTICLE

In vivo detection and automatic analysis of GABA in the mouse brain with MEGA-PRESS at 9.4 T

Jia Guo¹  | Zhu Gang² | Yanping Sun³ | Andrew Laine¹ | Scott A. Small⁴ | Douglas L. Rothman⁵ 

¹Department of Biomedical Engineering, Columbia University, New York, NY, USA

²Bruker BioSpin, Billerica, MA, USA

³Herbert Irving Comprehensive Cancer Center, Columbia University Medical Center, New York, NY, USA

⁴Departments of Neurology, Radiology, and Psychiatry, Columbia University College of Physicians and Surgeons, New York, NY, USA

⁵Departments of Diagnostic Radiology and Biomedical Engineering, Yale University, New Haven, CT, USA

Correspondence

D. L. Rothman, Departments of Diagnostic Radiology and Biomedical Engineering, Yale University, New Haven, CT 06510, USA.
Email: douglas.rothman@yale.edu

S. A. Small, Departments of Neurology, Radiology, and Psychiatry, Columbia University College of Physicians and Surgeons, New York, NY 10032, USA.
Email: sas68@columbia.edu

Funding information

National Institute of Health, Grant/Award Number: 5R01MH109159-02

The goals of this study were to develop an acquisition protocol and the analysis tools for Meshcher–Garwood point-resolved spectroscopy (MEGA-PRESS) in mouse brain at 9.4 T, to allow the *in vivo* detection of γ -aminobutyric acid (GABA) and to examine whether isoflurane alters GABA levels in the thalamus during anesthesia. We implemented the MEGA-PRESS sequence on a Bruker 94/20 system with ParaVision 6.0.1, and magnetic resonance spectra were acquired from nine male wild-type C57BL/6 J mice at the thalamus. Four individual scans were obtained for each mouse in a 2-h time course whilst the mouse was anesthetized with isoflurane. We developed an automated analysis program with improved correction for frequency and phase drift compared with the standard creatine (Cr) fitting-based method and provided automatic quantification. During MEGA-PRESS acquisition, a single voxel with a size of $5 \times 3 \times 3 \text{ mm}^3$ was placed at the thalamus to evaluate GABA to Cr (GABA/Cr) ratios during anesthesia. Detection and quantitative analysis of thalamic GABA levels were successfully achieved. We noticed a significant decrease in GABA/Cr during the 2-h anesthesia (by linear regression analysis: slope < 0 , $p < 0.0001$). In summary, our findings demonstrate that MEGA-PRESS is a feasible technique to measure *in vivo* GABA levels in the mouse brain at 9.4 T.

KEYWORDS

anesthesia, GABA, *J*-difference editing, magnetic resonance spectroscopy, MEGA-PRESS, mouse, quantification, thalamus

1 | INTRODUCTION

γ -Aminobutyric acid (GABA) is the primary inhibitory neurotransmitter in the human brain. A variety of studies of neurological and psychiatric disorders have shown its unique pathological characteristics in brain dysfunction.^{1,2} Amongst a wide range of methods for the measurement of GABA *in vivo*, Meshcher–Garwood point-resolved spectroscopy (MEGA-PRESS) is currently the most widely used magnetic resonance spectroscopy (MRS) technique.³ MEGA-PRESS is a *J*-difference editing (*JDE*) pulse sequence that separates GABA from overlapping metabolites, such as creatine (Cr), which is present in a much greater concentration. This separation is based on the selective induction and suppression of *J*-modulation of the GABA-H4 resonance.⁴

¹H MRS spectral editing of GABA with MEGA-PRESS is seeing increasing popularity in human studies thanks to the recent implementation of standard pulse sequences and processing algorithms. Nevertheless, in pre-clinical studies, mouse models continue to play a significant role in the scientific investigation of neuropsychiatric disorders. However, unlike for human studies, there has been a lack of similar standardization for animal studies. As yet, MEGA-PRESS has not been applied to *in vivo* mouse studies, although it has been implemented in a rat study.⁵ With the continued

Abbreviations used: Cho, choline; Cr, creatine; CSF, cerebrospinal fluid; FID, free induction decay; FWHM, full width at half-maximum; GABA, γ -aminobutyric acid; Glx, glutamate/glutamine; IACUC, Institutional Animal Care and Use Committee; *JDE*, *J*-difference editing; MEGA-PRESS, Meshcher–Garwood point-resolved spectroscopy; MM, macromolecules; MRI, magnetic resonance imaging; MRS, magnetic resonance spectroscopy; NA, number of averages; NAA, *N*-acetylaspartate; NIH, National Institutes of Health; RF, radiofrequency; SD, standard deviation; SNR, signal-to-noise ratio; STEAM, stimulated echo acquisition mode; tCr, total creatine; VAPOR, variable power and optimized relaxation delays

development of transgenic mouse models of human brain disease, there is an increasing need to measure and analyze GABA-edited MR spectra in mice routinely. There are several factors that have limited *in vivo* MEGA-PRESS studies in mice, including the small size of the mouse brain, increased respiratory motion and main magnet field drift (which can interfere with the editing sequence), the impact of anesthesia on brain metabolites (which can obscure the pathological changes being studied) and the lack of automated spectral processing and quantification software.

In the present study, we evaluate the feasibility and utility of MEGA-PRESS at 9.4 T for the detection of regional (thalamic) GABA content in the mouse brain. To deal with issues related to motion and main magnet field drift in MEGA-PRESS acquisition, we implemented a novel approach for automatic frequency and phase drift correction, as well as spectral quality determination. Sensitivity limitations were addressed through the use of a 9.4-T animal magnetic resonance imaging (MRI) system. MEGA-PRESS was implemented on the 9.4-T animal MRI system according to well-accepted sequence schemes proposed previously.^{6,7} The implemented sequence was first tested with phantom studies, which achieved high spectral quality and nearly optimal editing efficiency. We then investigated the effect of isoflurane on GABA levels in the mouse thalamus to further validate the successful implementation of MEGA-PRESS for *in vivo* mouse brain studies. Our studies replicated findings from previous small animal studies,^{8,9} which have shown that the GABA level is affected during anesthesia; compared with wakefulness, the GABA level was decreased significantly in the brain.

Overall, our results demonstrate that high-quality spectra can be reliably obtained and processed automatically from the mouse brain, opening up the use of MEGA-PRESS for *in vivo* MRS studies of transgenic mouse models of neurological and psychiatric disease.

This article does not cover the alternative acquisition schemes for GABA measurement, which include two-dimensional *J*-resolved MRS,^{10,11} short-TE stimulated echo acquisition mode (STEAM),^{12,13} unedited spectra at high field¹⁴ or other editing sequences.¹⁵

2 | EXPERIMENTAL DETAILS

Experiments were performed following the National Institutes of Health (NIH) guidelines and were approved by the Institutional Animal Care and Use Committee (IACUC).

2.1 | MEGA-PRESS sequence setup

A Bruker BioSpec 94/20 (field strength, 9.4 T; bore size, 20 cm) horizontal small animal MRI scanner with software ParaVision 6.0.1 (Bruker BioSpin, Billerica, MA, USA) and a 23-mm ¹H circularly polarized transmit/receive capable mouse head volume coil were used for the experiments. MEGA-PRESS allows GABA to be separated from the stronger overlying resonances of Cr and macromolecules (MM) by taking advantage of known *J*-couplings within their molecules. As a JDE technique, MEGA-PRESS involves the collection of two interleaved datasets which differ in their treatments of the GABA spin system. In one dataset, a refocusing pulse is applied to GABA spins at 1.9 ppm to selectively refocus the evolution of *J*-coupling to the GABA spins at 3 ppm (referred to as 'On'). In the other, the refocusing pulse is applied at 7.5 ppm so that the *J*-coupling evolves freely throughout the TE (referred to as 'Off').

MEGA-PRESS frequency-selective 180° refocusing pulses were applied at the offset of 1.9 ppm during the 'On' and 7.5 ppm during the 'Off' excitation with TE = 68 ms and TR = 2000 ms. As suggested previously,⁷ to minimize phase accumulation and to maximize editing efficiency, the following conditions on time delays must be satisfied to achieve the optimal signal detection: $t_2 = t_3 = t_4 = t_1 + t_5 = TE/4 = 17$ ms, as shown in Figure 1. The initial TE, twice t_1 , was kept as short as possible to ensure the adequate length of refocusing pulses. A Shinnar–LeRoux pulse of 28 ms duration and 98 Hz (0.245 ppm) full width at half-maximum (FWHM) was used for frequency-selective 180° refocusing. Spoiler gradients of 660 mT/m were applied for 1 ms, similar to the scheme proposed previously.⁶ Phantom studies validated the successful implementations of radiofrequency (RF) pulses, gradients and the choices of other sequence parameters, with the results demonstrated in Figure 2. For acquisition, 4096 points were acquired in 820 ms (with a bandwidth of 4.1 kHz corresponding to 10.25 ppm). The proposed ParaVision 6.0.1 MEGA-PRESS sequence is freely available upon reasonable request.

The majority of peaks in the spectrum are unaffected by the editing pulses, and so the subtraction of the refocused 'On' spectrum from the non-refocused 'Off' spectrum removes the unaffected peaks from the spectrum and retains only the peaks that are affected by the editing pulses. The *in vivo* edited spectrum contains signals close to 1.9 ppm (those directly affected by the pulses), the GABA signal at 3 ppm (coupled to GABA spins at 1.9 ppm), the combined glutamate/glutamine (Glx) peaks at 3.75 ppm (coupled to the Glx resonances at approximately 2.1 ppm) and MM peaks (coupled to the MM resonances at approximately 1.72 ppm). This process is demonstrated in Figure 3B. The 'On' and 'Off' spectra were collected in an interleaved fashion to limit the impact of subject and hardware instabilities. After correction for frequency and phase drift, as described below, subtraction and spectrum quantification were performed.

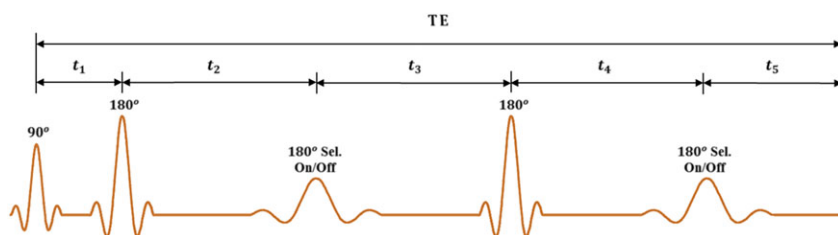


FIGURE 1 Representative Meshcher–Garwood point-resolved spectroscopy (MEGA-PRESS) pulse sequence

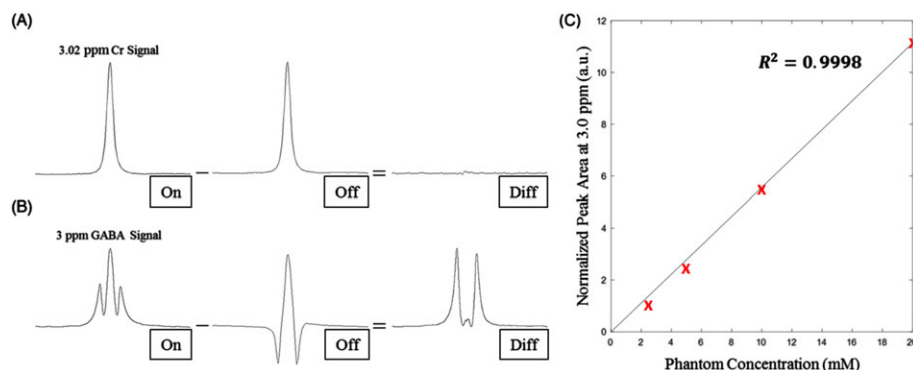


FIGURE 2 *In vitro* results of Meshcher–Garwood point-resolved spectroscopy (MEGA-PRESS) editing for γ -aminobutyric acid (GABA) solutions. (A) Effect of the editing pulses on the creatine (Cr) signal at 3.02 ppm. (B) Effect of the editing pulses on the GABA signal at 3 ppm. (C) GABA peak area versus GABA concentration

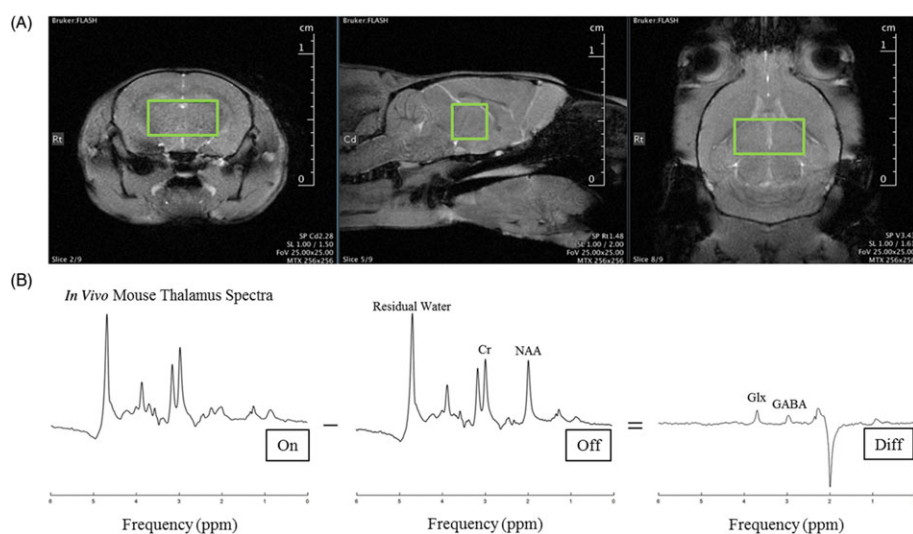


FIGURE 3 *In vivo* results of Meshcher–Garwood point-resolved spectroscopy (MEGA-PRESS) editing for the mouse thalamus. (A) Voxel placement at the mouse thalamus. (B) Representative diagrams of *in vivo* MEGA-PRESS editing at the mouse thalamus. Cr, creatine; GABA, γ -aminobutyric acid; Glx, glutamate/glutamine; NAA, *N*-acetylaspartate

2.2 | MEGA-PRESS acquisition

2.2.1 | *In vitro* phantom study

In order to verify the performance of the implemented MEGA-PRESS sequence, a series of phantom samples consisting of Cr or GABA in gadolinium-doped water were prepared at four different concentrations (2.5, 5, 10 and 20mM). Gadolinium-doped distilled water was prepared with Gadodiamide (Omniscan; GE Healthcare, Princeton, NJ, USA) at a concentration of 3.33 μ M. A 15-mL falcon tube was used to store the phantom solution because of its similar cross-sectional diameter to the mouse brain, which matched the 23-mm mouse head volume coil used for the *in vivo* animal study.

Single-voxel MEGA-PRESS spectra were acquired from a $6 \times 6 \times 6$ -mm³ voxel inside the phantom sample. For placement of the voxel, the manufacturer-provided multi-slice localizer scan was acquired. Following placement of the single voxel on each phantom sample, the manufacturer-provided field map-based shim method was used to adjust the shim currents. Nonlinear shimming up to the third order was obtained for the single voxel (with the shimming volume same as the acquired single voxel). Because linear terms in the higher order shim coils were not completely canceled out in the shim system, calibration of additional linear shimming was performed after the field map shim using a localized volume to maximize the area under the water free induction decay (FID) envelope. To ensure that the water frequency had no offset, one more round of voxel water frequency adjustment was applied. For linear shimming and water frequency adjustment, the manufacturer-provided protocols 'local shimming' and 'local frequency' were applied, respectively. After shimming and water ¹H frequency adjustment, water suppression was manually adjusted for each sample using variable power and optimized relaxation delays (VAPOR). During the MEGA-PRESS acquisition for each phantom sample, a total of 128 averages with 4096 points per average were obtained (64 'On' averages and 64 'Off' averages) with a scan time of 4 min and 16 s.

2.2.2 | *In vivo* animal study

The animals studied consisted of nine healthy adult male wild-type C57BL/6 J mice (age, 90 ± 5 days; body weight, 22 ± 3 g). During MR scans, the mice were anesthetized with inhaled isoflurane (1.8% mixture with medical air; adjusted as a dose range between 1% and 2%). We chose to use room air as opposed to O₂ to minimize physiological changes during anesthesia. The concentration of isoflurane was adjusted during the procedure to maintain the respiration rate in the range of 30–50 breaths/min. A flowing water heating pad was used to maintain the body temperature at around 37°C. Sterile eye lubricant was applied after each scan. All scans were performed in the late afternoon.

Single-voxel MEGA-PRESS spectra were acquired from the thalamus with a voxel size of $5 \times 3 \times 3$ mm³. The Allen Brain Atlas was used as the reference for the placement of the voxel to ensure that it was placed on and entirely captured the thalamus. The representative images demonstrating the voxel placement at the thalamus are illustrated in Figure 3A. Time course studies conducted previously⁸ have shown that, compared with wakefulness, isoflurane decreases GABA levels in the cat pontine reticular formation, and become stable 2 h after dialysis probe insertion. In our study, to keep track of the changes in thalamic GABA levels, four individual scans were acquired per mouse in a 2-h time course whilst the mouse was anesthetized with isoflurane. The first MEGA-PRESS scan for each mouse (immediately after the induction of isoflurane when all physiology monitors were in place) was defined as the initial level.

For placement of the voxel, a multi-slice localizer was acquired in 4 min and 36 s (TE = 3.447 ms; TR = 15 ms; field of view, 25×25 mm²; matrix, 256×256 ; five slices with 100 μ m thickness for each of the three orthogonal directions). To achieve consistent voxel placement for each animal, the position of the single voxel was carefully set up for the first mouse of the *in vivo* study using the Allen Brain Atlas as the reference. The slice that went through the middle section of the mouse brain was selected as the anatomical scan for voxel placement in each orientation. For the coronal slice (Figure 3A, left), the voxel was placed with its long edges perpendicular to the sagittal plane (the boundary between two hemispheres) of the brain, with the upper long edge placed below the hippocampus and the lower long edge above the third ventricle. For the axial slice (Figure 3A, right), the voxel was placed with its long edges perpendicular to the sagittal plane, with the upper long edge placed below the subfornical organ, the lower long edge above the dentate gyrus and the short edges reaching towards the medial boundary of the hippocampus on both sides. For the sagittal slice (Figure 3A, middle), the voxel was placed parallel to the ventral side of the brain. The single voxel position/geometry from the first mouse was further applied to all other mice. As each mouse was positioned at the same location inside the scanner (adjusted by the Bruker AutoPac) with the same body position (ventral side up), and there was only a small variation in their body sizes, only minimal voxel geometry adjustment was needed. Following placement of the single voxel, field map-based nonlinear shimming, linear shimming, water ¹H frequency adjustment and water suppression were performed. These corrections were again performed at the start of each subsequent scan to readjust the scanner frequency drift and to ensure optimal signal detection. Shimming was considered to be successful if FWHM of the unsuppressed water was below 25 Hz (0.0625 ppm). Water suppression using VAPOR was manually optimized. A total of 640 averages with 4096 points per average were obtained (320 'On' and 320 'Off') for an acquisition time of 21 min and 20 s per scan. Water reference scans were acquired in a single shot before each acquisition.

2.3 | Spectral processing and analysis

Bruker MEGA-PRESS spectroscopy raw data were processed in MATLAB 2015b (MathWorks, Natick, MA, USA). Original non-processed time-domain free induction decays (FIDs) were loaded from file 'rawdata.job0' stored in each study folder under the Bruker Paravision data directory. After loading FIDs, the first 68 points (Bruker default) of each transient of all repetitions were removed to correct for the digitization group delay. A line broadening value of 12 Hz (0.03 ppm) was used (which provides a similar line broadening extent to a human study at 3 T). A fast Fourier transformation was applied with zero filling to 2¹⁵ data points. Before running further analysis, we directly averaged every four consecutive 'On' or 'Off' spectra, respectively [i.e. number of averages (NA) = 4], to gain the spectral signal-to-noise ratio (SNR). The spectra used for frequency and phase drift correction and spectral fitting had 80 'On' and 80 'Off' spectra, respectively.

2.3.1 | Development and implementation of improved frequency and phase drift correction

A major limitation in JDE pulse sequences is that they depend on the subtraction of spectra to reveal the edited resonance. As a result of the overlapping resonances being an order of magnitude larger in intensity than the GABA resonance, small changes in scanner frequency and spectral phase will lead to incomplete subtraction and distortion of the edited spectrum. The standard approach in GABA editing is to apply frequency and phase drift correction of individual frequency domain transients^{4,5,16} by fitting the Cr signal at 3 ppm. The major limitation of the Cr fitting-based correction method is that it relies strongly on sufficient SNR of the Cr signal in the spectrum.

To overcome this limitation, we tried to correct the frequency drift over a larger spectral frequency range. Instead of adjusting the frequency drift by fitting the single Cr peak at 3 ppm, we independently aligned each 'Off' power spectrum to the median 'Off' power spectrum (as the reference) by maximizing their cross-correlation over a frequency range of 1.5–4.5 ppm. The frequency range was selected to avoid the unstable residual water signal. The power spectrum was used for frequency drift correction because it was independent of the spectral phase. The frequency drift correction was implemented by modifying the open-source MATLAB program *icoshift*,¹⁷ where we used the 'Off' power spectrum as the program input and the median 'Off' power spectrum as the correction reference, and set the piece-wise correction intervals to a single spectral interval in the range of 1.5–4.5 ppm.

Phase drifts between transients also lead to subtraction error. These shifts can arise from animal motion, which creates field shifts that are not balanced out on either side of the spin echo portion of the sequence, or from the motion of magnetic objects within the magnetic stray field (which was not observed in our study). The phase drift correction accuracy also depends on SNR. To achieve accurate phase drift correction given the SNR available, we used the algorithm ACME, proposed by Chen et al.¹⁸ This is the first time that ACME has been applied in this context to process JDE spectra. In ACME, phase drift correction was achieved by minimizing the spectral entropy, with the probability distribution used in the entropy function defined as the normalized second derivative of the spectrum. ACME was shown to be able to correct the spectral phase effectively even in the presence of considerable noise.¹⁸ Phase drift correction was also performed over the frequency range of 1.5–4.5 ppm independently at each 'Off' transient. Only the zero-order phase term was considered when solving the energy function and the first-order phase of the spectrum was fixed to zero because the correct timing of the data acquisition window in the PRESS sequence had been validated through phantom experiments (where no first-order phase was observed in the phantom spectra). The phase drift correction was implemented using the open-source MATLAB program ACME.¹⁸

The same frequency and phase drift correction was applied to the corresponding 'On' spectrum. After the correction, time averaging was performed and the edited difference spectrum was calculated.

Compared with the standard method – the Cr fitting-based correction method – the proposed method is referred to as the 'unsupervised spectral-based correction method' in this article.

2.3.2 | Outlier rejection

Time-resolved spectra were excluded before time averaging on the basis of being greater than three standard deviations (SDs) from the mean in any one of the following metrics: the cross-correlation to reference, the frequency shift and the zero-order phase. Rejections were applied in a pairwise manner.

2.3.3 | Spectral fitting

Spectral fitting was achieved using the modeling algorithms proposed by the Gannet pipeline,¹⁶ where the edited GABA signal at 3 ppm or the co-edited Glx signal at 3.75 ppm was fitted as a linear combination of the linear baseline and a single Gaussian peak, and the Cr and choline (Cho) signals were fitted as a linear combination of the linear baseline and the sum of two Lorentzian peaks. Fitting of the unsuppressed water peak was achieved using a single Gaussian-Lorentzian peak. The fitted Gaussian or Lorentzian peak area was used for the quantification of each metabolite. The simple single-Gaussian model adopted by Gannet for GABA quantification appears to be sufficient for typical MEGA-PRESS data, considering the somewhat competing demands of parsimony and robustness.¹⁶ Through spectral fitting, in addition to generating the metabolite levels as the areas under the best-fit model peaks, the fitting errors were also calculated. The fitting error was generated as the normalized residual¹⁶ for each fit, i.e. the SD of the fitting residual divided by the amplitude of the fitted peak.

In summary, the proposed MATLAB program consists of two main modules: the data loading module, which reads the Bruker time-domain raw data and processes it into a frequency-domain GABA-edited spectrum with frequency and phase drift correction; the spectral fitting module, which quantifies the metabolite concentrations, including non-edited *N*-acetylaspartate (NAA), Cr, Cho and unsuppressed water, as well as edited GABA and Glx. The proposed MATLAB program is also freely available upon reasonable request.

2.3.4 | Statistical analysis

We used GABA/Cr to estimate the *in vivo* GABA levels. The GABA concentration was normalized to the Cr concentration from the same voxel to reduce inter-subject variance caused by differences in global signal strength and cerebrospinal fluid (CSF) fraction within the voxel. Linear regression analysis was performed to test whether there was a linear relationship between the changes in GABA/Cr (compared with the initial level) and the duration of anesthesia with isoflurane. We also compared GABA/Cr of the last time point with the initial level using a paired sample *t*-test (one-tailed) to determine whether there was a significant decrease in GABA levels after 2 h of anesthesia.

2.4 | Evaluation and comparison of proposed method and Cr fitting-based method for frequency and phase drift correction

To examine the difference between the Cr fitting-based correction and the proposed method quantitatively, we compared the performance of the Cr fitting-based correction and the unsupervised spectral-based correction at various SNR levels, using a simulated spectrum with given frequency and phase drifts.

A simulated mouse brain 'Off' mode spectrum was generated as a linear combination of simulated metabolite bases to approximate the major peaks of the *in vivo* mouse spectrum in the frequency range of 1.5–4.5 ppm. The metabolite basis set included simulated NAA, Cr and Cho signals. First, metabolite bases with the same spectral parameters as the *in vivo* data (TE = 68 ms; 2¹⁵ data points; spectral width = 4.1 kHz; FWHM = 12 Hz (0.03 ppm); RF offset = 4.79 ppm; field strength = 400 MHz) were simulated for NAA, Cr and Cho, using the 'LCM basisset' module of the MATLAB toolkit NMRWizard.¹⁹ Second, the *in vivo* mouse brain 'Off' mode FID data acquired from a single subject were fitted with the simulated metabolite basis set, as a sum of exponentially damped sinusoids in the time domain, using an in-house MATLAB implementation of the spectral fitting algorithm VARPRO.²⁰ Finally, we took the fitting result in the frequency domain as the simulated, noise-free 'Off' spectrum (Figure 5, see later).

Pre-defined frequency or phase drift was added independently to the simulated noise-free 'Off' spectrum S to simulate a drifted noise-free spectrum S' . The frequency errors, $f(i) = \left(\frac{i}{100}\right) \times 40 \text{ Hz} - 20 \text{ Hz}$, $i \in \{0, 1, 2, \dots, 100\}$, were defined as 101 evenly spaced frequency drifts between -20 Hz and $+20 \text{ Hz}$. The phase errors, $\varphi(i) = \left(\frac{i}{100}\right) \times 60^\circ - 30^\circ$, $i \in \{0, 1, 2, \dots, 100\}$, were defined as 101 evenly spaced phase drifts between -30° and $+30^\circ$. These terms were chosen to cover the frequency or phase drift ranges observed in the *in vivo* experiments (Table 1). To approximate a range of different SNR conditions, normally distributed zero-mean random noises were added to both the original spectrum S and the drifted spectrum S' , with SNR values (measured as the Cr peak amplitude divided by the SD of the added noise in the frequency domain) of 20, 10, 5 and 2.5. At each SNR, 10 simulated datasets were generated for each frequency or phase drift. The frequency or phase drift correction was performed on each dataset using the Cr fitting-based correction method, as well as the unsupervised spectral-based correction method. To evaluate the performance, we measured the frequency and phase estimation errors at the four different SNRs for each method. The estimation error was defined as the absolute difference between the estimated drift and the actual drift.

3 | RESULTS

3.1 | *In vitro* phantom experiment

In vitro phantom results are demonstrated in Figure 2. The expected spectral shapes (from the 'On', 'Off' and 'Diff' spectra) were observed for both Cr and GABA phantoms, as shown in Figure 2A, B. A GABA editing efficiency of 49.45% was achieved using a 50mM GABA solution. The editing efficiency was defined as half of the ratio between the areas under the GABA peaks at 3 ppm in the 'Diff' spectrum to the areas under the GABA peaks at 3 ppm in the refocused 'On' spectrum (with 50% indicating perfect editing). Excellent agreement between the GABA concentrations determined analytically and the detected GABA signals at 3 ppm from the 'Diff' spectrum was noted, with the squared correlation coefficient $R^2 > 0.999$ as shown in Figure 2C.

3.2 | *In vivo* animal experiment

Figure 3A illustrates the voxel placement at the mouse thalamus for MEGA-PRESS acquisition in horizontal, sagittal and coronal sections. Figure 3B shows the typical *in vivo* spectra acquired from the thalamus of a single subject in our study. Consistently high spectral quality and high sensitivity to GABA were achieved for all the spectra.

The quality of the *in vivo* data collected was determined using per-average SNR values of the 'Off' spectra after frequency and phase corrections. The signal was calculated as the metabolite peak amplitude of Cr, and the noise was calculated as the SD of the first 5000 data points at the frequency range of 8.2–9.8 ppm. The frequency drift and phase drift were also reported as a way to quantify scan stability. Table 1 lists the minimum per-average SNRs (calculated after averaging every four consecutive spectra with $NA = 4$), and also reports maximum drifts (determined using the proposed method). The results are reported as the mean \pm SD for each time point across nine subjects.

Figure 4 shows the results of the averaged 'Off' and 'Diff' spectrum from one mouse, without frequency and phase drift correction (Figure 4A, B), their corresponding results of the Cr fitting-based correction method and the results of our proposed method (Figure 4C, D). The proposed method gave better frequency and phase drift correction and smaller subtraction errors compared with the results using the standard Cr fitting-based correction. The edited spectrum of the proposed method showed a better improvement on the GABA SNR and linewidth.

Figure 5 shows the simulated 'Off' spectrum in the frequency range of 1.5–4.5 ppm overlapped with the *in vivo* 'Off' spectrum acquired from a single subject.

Figure 6A, B shows examples of the simulated spectrum with an SNR of 20 and the same spectrum with a frequency drift and a phase drift. Figure 6C, D shows the same spectrum, following frequency and phase drift correction using our proposed method.

Figure 7A, B shows the drift correction estimation errors of the Cr fitting-based correction method and the unsupervised spectral-based correction method, respectively, at four SNR levels. Each bar represents the average error across 10 simulated datasets for all 101 drifts. For simulated datasets with SNRs of 20, 10, 5 and 2.5, the frequency estimation errors were 0.34, 0.60, 1.41 and 3.59 Hz, respectively, for the Cr fitting-based correction method; and 0.18, 0.38, 0.77 and 1.83 Hz, respectively, for the proposed method. The phase estimation errors were

TABLE 1 The minimum per-average signal-to-noise ratios (SNRs) and the maximum drifts (determined by our proposed method) of the *in vivo* spectra. Data are reported as the mean \pm standard deviation (SD) for each time point across nine subjects

	Minimum SNR	Maximum frequency drift (Hz)	Maximum phase drift (deg)
Time 1	8.49 \pm 1.08	9.51 \pm 5.88	19.25 \pm 7.99
Time 2	8.55 \pm 0.89	3.58 \pm 1.97	15.87 \pm 10.12
Time 3	8.89 \pm 1.42	3.69 \pm 4.04	15.02 \pm 7.84
Time 4	8.53 \pm 1.48	2.49 \pm 2.17	13.33 \pm 6.121

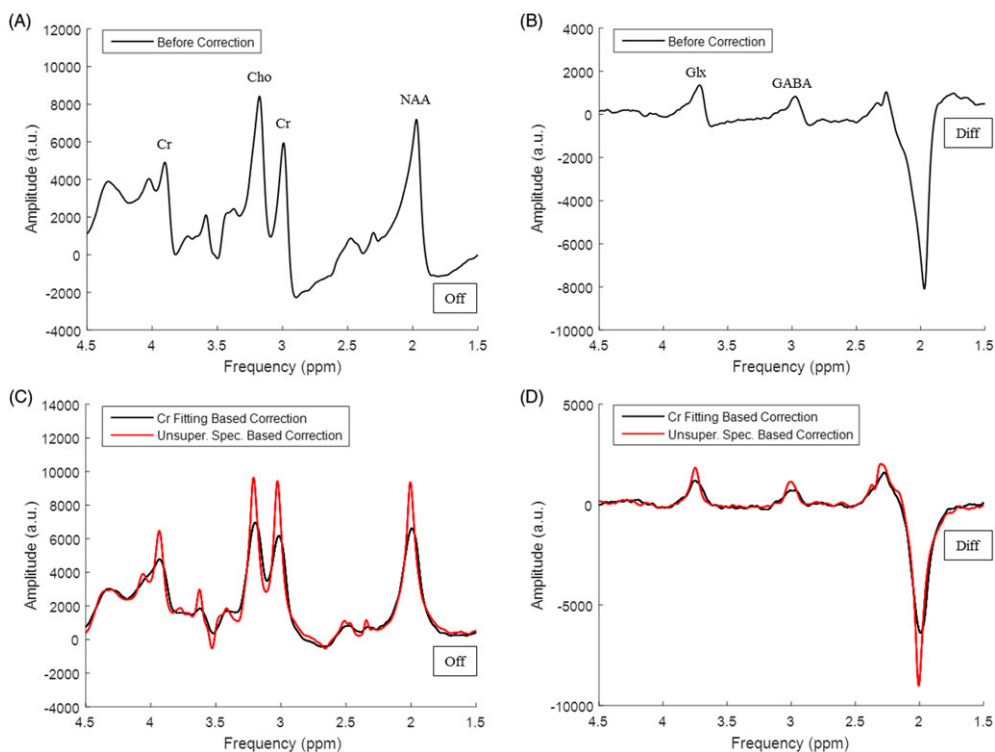


FIGURE 4 Comparison of frequency and phase drift correction methods. (A) Averaged 'Off' spectrum from one scan of a single subject without correction. (B) Averaged 'Diff' spectrum from one scan of a single subject without correction. (C) Averaged 'Off' spectrum after frequency and phase correction using the creatine (Cr) fitting-based method (black line) and the proposed method (red line). (D) Averaged 'Diff' spectrum after frequency and phase correction using the Cr fitting-based method (black line) and the proposed method (red line). Cr, creatine; Cho, choline; GABA, γ -aminobutyric acid; Glx, glutamate/glutamine; NAA, N-acetylaspartate

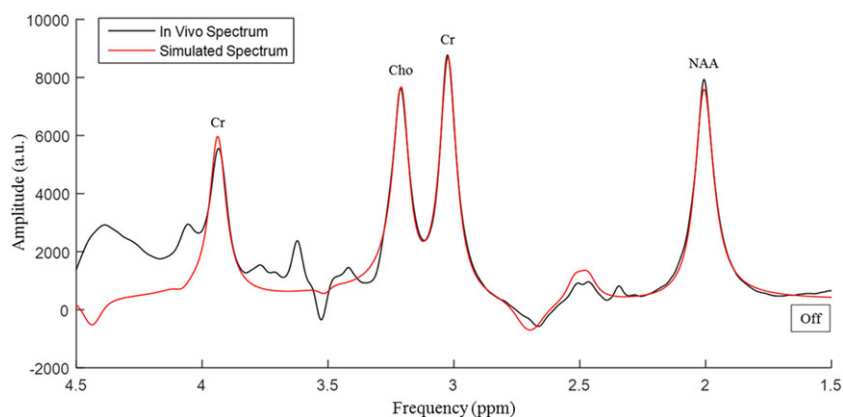


FIGURE 5 Simulated spectrum (red line) to approximate a noise-free version of the *in vivo* 'Off' spectrum (black line). Cr, creatine; Cho, choline; NAA, N-acetylaspartate

3.11°, 6.56°, 13.15° and 29.75°, respectively, for the Cr fitting-based correction method; and 1.07°, 1.98°, 2.68° and 3.89°, respectively, for the proposed method.

Figure 8A plots the time course of *in vivo* thalamic GABA levels during anesthesia. The graph shows continuous decays in GABA/Cr within the 2-h scan session. A significant decrease (slope < 0; $p = 1.28\text{e-}09$) of GABA/Cr can be observed from the linear regression analysis. We also compared GABA/Cr of the last time point with the initial level using a paired sample *t*-test (Figure 8B), and a significant 37.6% decrease ($p < 0.0001$) in GABA/Cr was observed. Table 2 lists the estimated GABA and Cr peak areas, the GABA/Cr levels, the FWHMs and the fitting errors of the GABA and Cr peaks for the *in vivo* spectra. Data are reported as the mean \pm SD for each time point across nine subjects.

Supporting Information Figure S1 summarizes the output reports for one subject. Separate reports are saved for both the data loading step (Figure S1A) and the spectral fitting step (Figure S1B, C). Both graphical and quantitative results are displayed in the reports, which allow the user to access data and fitting quality. In the data loading report, details of frequency and phase drift correction are displayed. In the spectral fitting report, the estimated metabolite areas and fitting errors are listed for GABA, Glx and Cr.

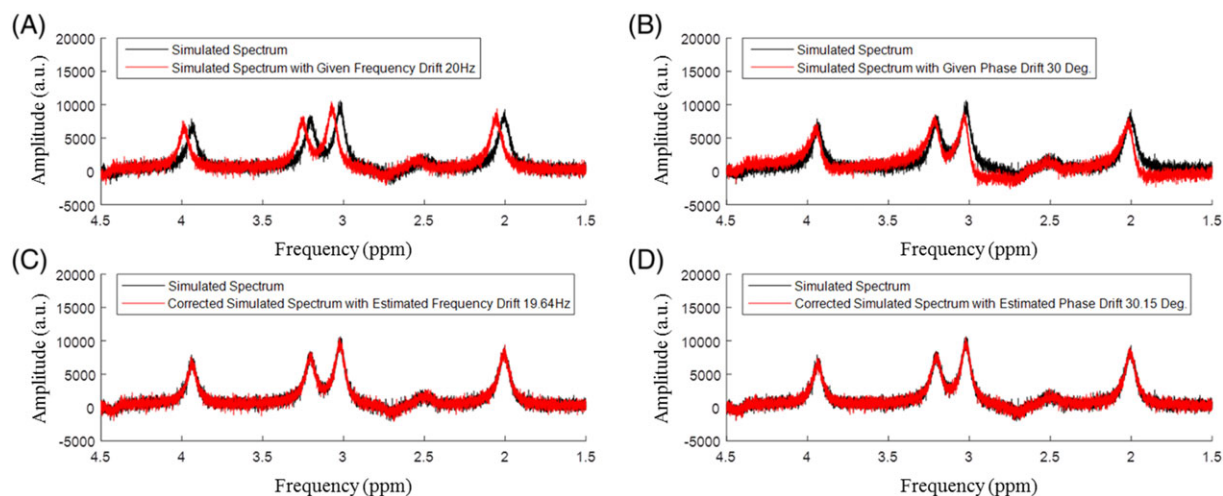


FIGURE 6 Frequency and phase drift correction using the proposed unsupervised spectral-based correction at a signal-to-noise ratio (SNR) of 20. (A) Simulated 'Off' spectrum (black line) and the same spectrum plus a frequency drift of 20 Hz (red line). (B) Simulated 'Off' spectrum (black line) and the same spectrum plus a phase drift of 30° (red line). (C) Simulated 'Off' spectrum (black line) and the frequency drift-corrected spectrum with an estimated frequency drift of 19.64 Hz (red line). (D) Simulated 'Off' spectrum (black line) and the phase drift-corrected spectrum with an estimated phase drift of 30.15° (red line)

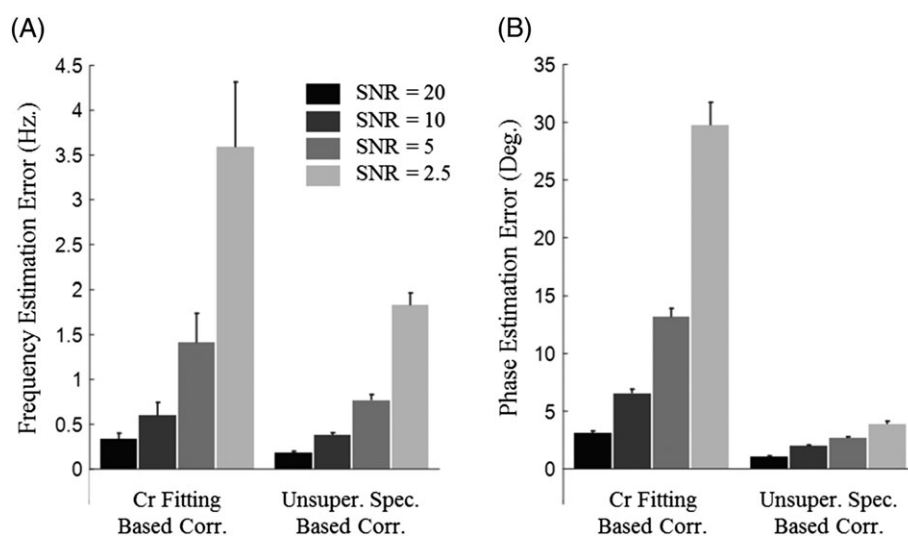


FIGURE 7 Comparison between the proposed unsupervised spectral-based correction and the standard creatine (Cr) fitting-based correction method. (A) Bar graph showing the frequency estimation error (in Hz) and its standard deviation of the Cr-based method and the proposed method. SNR, signal-to-noise ratio. (B) Bar graph showing the phase estimation error (in degree) and its standard deviation of the Cr-based method and the proposed method

4 | DISCUSSION

The consistently high quality and sensitivity to GABA observed for all spectra from each mouse indicates the feasibility of MEGA-PRESS in mice at 9.4 T in combination with automated frequency and phase drift correction and spectral fitting of GABA.

In vivo MRS commonly has frequency and phase drift problems during the acquisition of spectra. These problems, if not addressed properly, can result in spectral lineshape distortion and artifactual metabolite peak broadening in the spectrum. Our results suggest that the proposed unsupervised spectral-based correction method can accurately estimate both the frequency and phase drifts, and correct them, even at a considerably high noise level. We evaluated our proposed method by comparing it with the standard Cr fitting-based method. Specifically, we compared the ability of each method to accurately estimate the frequency and phase drifts in the simulated MR spectrum in which the drifts are known, and at various SNR levels. Our proposed method outperformed the Cr fitting-based correction method at all SNR levels tested. We noticed that the performance of the Cr fitting-based correction method is limited when the spectral SNR is smaller than 10, and the performance of the proposed method for drift correction is limited at the lowest SNR of 2.5 (when the spectrum is dominated by noise). For *in vivo* MEGA-PRESS data of mouse brain, the limited SNR puts the standard Cr fitting-based correction method at a disadvantage.

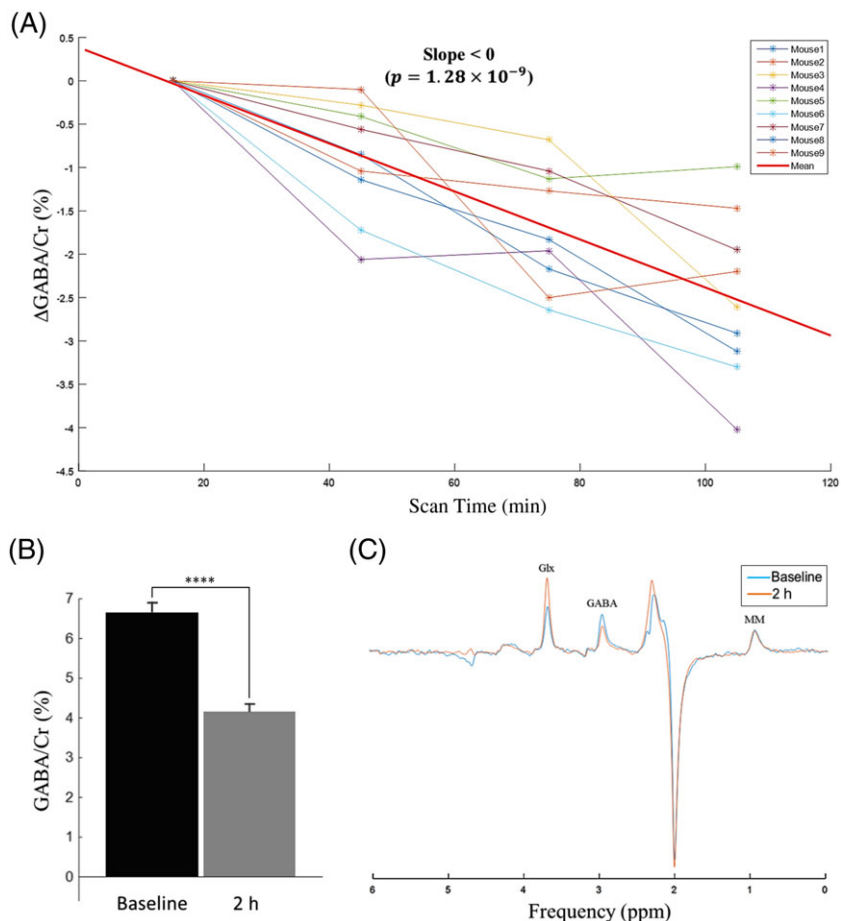


FIGURE 8 Time course for examination of the influence of isoflurane on γ -aminobutyric acid (GABA) levels at the mouse thalamus. (A) Linear regression analysis result. (B) Bar graphs of GABA to creatine (Cr) ratios at baseline and at 2 h post-anesthesia with Student's *t*-test result. (C) Overlaid display of the overall mean 'Diff' spectra across all subjects for baseline and 2 h post-anesthesia. Cr, creatine; Glx, glutamate/glutamine; GABA, γ -aminobutyric acid; MM, macromolecules

TABLE 2 The estimated γ -aminobutyric acid (GABA) and creatine (Cr) peak areas, GABA/Cr area ratios, full widths at half-maximum (FWHMs) for GABA and Cr peaks, and the fitting error for GABA and Cr peaks of the *in vivo* spectra. Data are reported as the mean \pm standard deviation (SD) for each time point across nine subjects

	GABA	Cr	GABA/Cr (%)	FWHM (GABA)	FWHM (Cr)	Fitting error (%) (GABA)	Fitting error (%) (Cr)
Time 1	58.04 \pm 7.83	871.11 \pm 59.19	6.66 \pm 0.76	14.30 \pm 4.19	15.68 \pm 3.01	6.88 \pm 2.02	2.21 \pm 0.41
Time 2	51.39 \pm 4.02	895.78 \pm 68.14	5.76 \pm 0.51	14.73 \pm 4.56	15.95 \pm 3.26	6.51 \pm 2.38	2.73 \pm 0.47
Time 3	44.80 \pm 5.58	909.89 \pm 80.51	4.97 \pm 0.84	14.69 \pm 6.68	15.71 \pm 4.13	6.26 \pm 3.14	2.95 \pm 1.04
Time 4	37.85 \pm 4.94	917.11 \pm 78.99	4.15 \pm 0.63	13.41 \pm 2.43	14.50 \pm 3.99	8.46 \pm 3.79	2.86 \pm 0.76

As discussed, before spectral averaging, we performed frequency and phase drift correction for each spectrum. In our study, the raw individual spectrum has a limited SNR (~ 4 – 5), which makes the correction method less accurate if we run the correction on the individual spectra directly. We directly averaged every four individual 'On' or 'Off' spectra, respectively, before frequency and phase correction, as these drifts for four adjacent spectra were negligible. This procedure doubled the SNR of the spectra used for frequency and phase correction, which provided a sufficient SNR (~ 8 – 10) for more accurate frequency and phase drift estimations.

Similar to our proposed method, a recently published method, spectral registration,²¹ is also able to overcome the limitations of the Cr fitting-based correction method by registering each spectrum with a reference spectrum to correct the frequency and phase drift in the time domain. As a supervised method, one characteristic of 'spectral registration' is that it requires a frequency and phase drift-free reference scan as the ground truth. In comparison, as an unsupervised method, our proposed approach operates in a fully automated fashion without additional information provided by the user. Another distinction is that our proposed approach for frequency and phase drift correction is a frequency domain algorithm.

All the observed data were processed using the in-house MATLAB-based program. GABA levels can be quantified relative to NAA, Cr, Cho or the unsuppressed water peak. In this study, we chose Cr as the internal reference, as it is considered to be stable.^{22,23} The Cr peak at 3 ppm sums together the very similar compounds creatine and phosphocreatine, which cannot be distinguished even at high magnetic field. Some studies refer to this as total creatine (tCr). The Cr peak also has the advantage over unsuppressed water as it was acquired simultaneously with GABA at the same voxel, so that Cr shares the same drift as GABA. Water quantification has excellent SNR and can provide absolute GABA concentration;

however, it requires tissue composition correction which accounts for the differences in the apparent water concentrations between white matter, gray matter and CSF, considering the variation in the voxel tissue composition between subjects. We consider this as part of our future work.

For the *in vitro* phantom MR spectrum, with a much narrower linewidth than the *in vivo* spectrum, fitting of the GABA signal using a simple single-Gaussian method is apparently not preferred. For the *in vivo* spectrum, where GABA has a wider linewidth, previous work¹⁶ has shown that there is no clear difference in the GABA fitting performance between the simple Gaussian model used by Gannet and the other more complex models presented, i.e. double-Gaussian, double-Lorentzian, etc. However, spectral fitting with the single-Gaussian model can become a limitation of the overall method when the *in vivo* GABA signal has a narrower linewidth. Some improvements in quantification may be possible using the simulated GABA resonances for GABA fitting instead of the simple single-Gaussian peak. We also consider this as part of our future work.

A Shinnar–LeRoux pulse with a duration of 28 ms and a FWHM of 98 Hz (0.245 ppm) was used for frequency-selective 180° refocusing. In our study, the refocusing bandwidth of the editing pulses was sufficiently narrow (0.245 ppm), such that the MM signal at 1.72 ppm was not significantly affected, which led to a minor MM contribution to the edited signal. However, to be conservative, we still referred to our signal as potentially including contributions from co-edited MM, and therefore refer to it as the field convention of GABA+. The achievement of a better MM suppression is part of our future work. The co-edited MM can be further reduced in future implementations through the use of MM suppression pulses and/or symmetric application of the refocusing pulse in the 'off' mode about the 1.72-ppm MM multiplet.^{24,25}

The time course results indicated a statistically significant reduction in thalamic GABA/Cr caused by isoflurane during standard anesthesia. Decreasing thalamic GABA levels may comprise one mechanism by which isoflurane causes loss of consciousness, which can be validated together with further studies on cortical excitability and muscular hypotonia to examine whether they co-vary with the GABA levels. Being able to scan awake mice²⁶ may allow for the capture of the changes in GABA during the induction of and recovery from isoflurane anesthesia, which is necessary to accurately quantify the difference in GABA levels between the awake and anesthetized conditions.

In conclusion, we have demonstrated the feasibility of MEGA-PRESS for the *in vivo* detection of GABA in mouse brain in combination with automated frequency and phase drift correction and spectral fitting. High-quality spectra can be acquired repeatedly within a reasonable scan time. We have also shown that GABA levels in the mouse thalamus are decreased significantly by isoflurane during anesthesia. To minimize the unintended anesthetic effect, the choice of anesthesia (including the type of anesthetic) should be considered for the *in vivo* mouse study on GABA.

ACKNOWLEDGEMENTS

This work was supported by 5R01MH109159-02. We thank Robin A. de Graaf for support of NMRWizard and discussions regarding this work. We thank Frank Provenzano and Cheng-Chia Wu for their thoughtful comments that improved the manuscript.

ORCID

Jia Guo  <http://orcid.org/0000-0003-4803-0279>

Douglas L. Rothman  <http://orcid.org/0000-0001-9321-4195>

REFERENCES

1. Wong GTC, Bottiglieri T, Snead CO III. GABA, g-hydroxybutyric acid, and neurological disease. *Ann Neurol*. 2003;6:3-12.
2. Brambilla P, Perez J, Barale F, Schettini G, Soares JC. GABAergic dysfunction in mood disorders. *Mol Psychiatr*. 2003;8:721-737. see also 715
3. Mullins PG, McGonigle DJ, O'Gorman RL, et al. Current practice in the use of MEGA-PRESS spectroscopy for the detection of GABA. *Neuroimage*. 2014;86:43-52.
4. Rothman DL, Petroff OA, Behar KL, Mattson RH. Localized ¹H NMR measurements of gamma-aminobutyric acid in human brain *in vivo*. *Proc Natl Acad Sci U S A*. 1993;90(12):5662-5666.
5. Sawiak SJ, Jupp B, Taylor T, Caprioli D, Carpenter TA, Dalley JW. *In vivo* γ-aminobutyric acid measurement in rats with spectral editing at 4.7T. *J Magn Reson Imaging*. 2016;43(6):1308-1312.
6. Mescher M, Merkle H, Kirsch J, Garwood M, Gruetter R. Simultaneous *in vivo* spectral editing and water suppression. *NMR Biomed*. 1998;11(6):266-272.
7. de Graaf RA, Rothman DL. Spectra editing. *eMagRes*. 2016;5:1147-1156.
8. Vanini G, Watson CJ, Lydic R, Baghdoyan HA. Gamma-aminobutyric acid-mediated neurotransmission in the pontine reticular formation modulates hypnosis, immobility, and breathing during isoflurane anesthesia. *Anesthesiology*. 2008;109:978-988.
9. Watson CJ, Lydic R, Baghdoyan HA. Sleep duration varies as a function of glutamate and GABA in rat pontine reticular formation. *J Neurochem*. 2011;118:571-580.
10. Jensen JE, Frederick BD, Wang L, Brown J, Renshaw PF. Two-dimensional, J-resolved spectroscopic imaging of GABA at 4 Tesla in the human brain. *Magn Reson Med*. 2005;54(4):783-788.
11. Ryner LN, Sorenson JA, Thomas MA. Localized 2D J-resolved ¹H MR spectroscopy: strong coupling effects *in vitro* and *in vivo*. *Magn Reson Imaging*. 1995;13(6):853-869.
12. Hu J, Yang S, Xuan Y, Jiang Q, Yang Y, Haacke EM. Simultaneous detection of resolved glutamate, glutamine, and γ-aminobutyric acid at 4T. *J Magn Reson*. 2007;185(2):204-213.
13. Thompson RB, Allen PS. Response of metabolites with coupled spins to the STEAM sequence. *Magn Reson Med*. 2001;45(6):955-965.

14. Mekle R, Mlynárik V, Gambarota G, Hergt M, Krueger G, Gruetter R. MR spectroscopy of the human brain with enhanced signal intensity at ultrashort echo times on a clinical platform at 3T and 7T. *Magn Reson Med*. 2009;61(6):1279-1285.
15. Choi IY, Lee SP, Shen J. In vivo single-shot three-dimensionally localized multiple quantum spectroscopy of GABA in the human brain with improved spectral selectivity. *J Magn Reson*. 2005;172(1):9-16.
16. Edden RA, Puts NA, Harris AD, Barker PB, Evans CJ. Gannet: a batch-processing tool for the quantitative analysis of gamma-aminobutyric acid-edited MR spectroscopy spectra. *J Magn Reson Imaging*. 2014;40(6):1445-1452.
17. Savorani F, Tomasi G, Engelsens SB. icoshift: a versatile tool for the rapid alignment of 1D NMR spectra. *J Magn Reson*. 2010;202(2):190-202.
18. Chen L, Weng ZQ, Goh LY, Garland M. An efficient algorithm for automatic phase correction of NMR spectra based on entropy minimization. *J Magn Reson*. 2002;158:164-168.
19. de Graaf RA, Chowdhury GM, Behar KL. Quantification of high-resolution (1)H NMR spectra from rat brain extracts. *Anal Chem*. 2011;83(1):216-224.
20. Van der Veen JW, de Beer R, Luyten PR, Van Ormondt D. Accurate quantification of in vivo ³¹P NMR signals using the variable projection method and prior knowledge. *Magn Reson Med*. 1998;6(1):92-98.
21. Near J, Edden RA, Evans CJ, Paquin R, Harris A, Jezzard P. Frequency and phase drift correction of magnetic resonance spectroscopy data by spectral registration in the time domain. *Magn Reson Med*. 2015;73(1):44-50.
22. Du F, Zhang Y, Iltis I, et al. In vivo proton MRS to quantify anesthetic effects of pentobarbital on cerebral metabolism and brain activity in rat. *Magn Reson Med*. 2009;62(6):1385-1393.
23. Boretius S, Tammer R, Michaelis T, Brockmöller J, Frahm J. Halogenated volatile anesthetics alter brain metabolism as revealed by proton magnetic resonance spectroscopy of mice in vivo. *Neuroimage*. 2013;69:244-255.
24. Behar KL, Rothman DL, Spencer DD, Petroff OA. Analysis of macromolecule resonances in ¹H NMR spectra of human brain. *Magn Reson Med*. 1994;32(3):294-302.
25. Henry PG, Dautry C, Hantraye P, Bloch G. Brain GABA editing without macromolecule contamination. *Magn Reson Med*. 2001;45(3):517-520.
26. Ferris CF, Kulkarni P, Toddes S, Yee J, Kenkel W, Nedelman M. Studies on the Q175 knock-in model of Huntington's disease using functional imaging in awake mice: evidence of olfactory dysfunction. *Front Neurol*. 2014;5:94

SUPPORTING INFORMATION

Additional Supporting Information may be found online in the supporting information tab for this article.

How to cite this article: Guo J, Gang Z, Sun Y, Laine A, Small SA, Rothman DL. In vivo detection and automatic analysis of GABA in the mouse brain with MEGA-PRESS at 9.4 T. *NMR in Biomedicine*. 2018;31:e3837. <https://doi.org/10.1002/nbm.3837>